The Geological Society of America
Special Paper 473
2011

Bedforms, coastal-trapped waves, and scour process observations from the continental shelf of the northern Black Sea

A. Trembanis*
S. Nebel
A. Skarke
Department of Geological Sciences, University of Delaware, 109 Penny Hall, Newark, Delaware 19716, USA

D.F. Coleman
R.D. Ballard
Graduate School of Oceanography, University of Rhode Island, South Ferry Road, Narragansett, Rhode Island 02882, USA

A. Yankovsky
Marine Science Program and Department of Geological Sciences, University of South Carolina, Columbia, South Carolina 29208, USA

I.V. Buynevich*
Geology & Geophysics Department, Woods Hole Oceanographic Institution, MS 22, Woods Hole, Massachusetts 02543, USA

S. Voronov
Department of Underwater Heritage, Institute for Archaeology, Academy of Sciences of Ukraine, Kyiv, Ukraine

ABSTRACT

The Black Sea basin presents an ideal laboratory for investigations of morphodynamic interplay between response (morphology) and force (processes) associated with shelf sedimentation. Recent studies along the perimeter of the basin have documented the existence of a complex, heterogeneous seafloor varyingly composed of sand, gravel, silt, and clay. Side-scan sonar data are utilized to establish the spatial patterns of bedform types in the area. In addition, a benthic tripod, configured with an acoustic Doppler current profiler, a rotary fanbeam sonar, and a conductivity-temperature sensor was deployed to record seabed dynamics in response to changing forcing conditions. Together, the tripod and side-scan survey data sets provide a complementary basis for deciphering the processes responsible for the observed seafloor morphology.

The side-scan sonar data allows for the determination of spatial patterns of bedform length and orientation. In total, 2376 individual large sand wave bedforms were

*E-mail, Trembanis—art@udel.edu; present address, Buynevich—Department of Earth and Environmental Science, Temple University, 1901 N. 13th Street, Philadelphia, Pennsylvania 19122, USA; coast@temple.edu.

Trembanis, A., Nebel, S., Skarke, A., Coleman, D.F., Ballard, R.D., Yankovsky, A., Buynevich, I.V., and Voronov, S., 2011, Bedforms, coastal-trapped waves, and scour process observations from the continental shelf of the northern Black Sea, *in* Buynevich, I.V., Yanko-Hombach, V., Gilbert, A.S., and Martin, R.E., eds., Geology and Geoarchaeology of the Black Sea Region: Beyond the Flood Hypothesis: Geological Society of America Special Paper 473, p. 165–178, doi: 10.1130/2011.2473(10).

digitized in geographic information systems with mean and modal wavelengths of 72.8 and 15.7 m respectively. The correlation of near-inertial waves (velocity amplitude 12–20 cm/s and period 12–16 h) and bedform geometry suggest that the extensive sand-wave patches imaged across the shelf are affected by active modern processes and may themselves be modern features or perhaps relict features that remain active presently. Progressive vector diagrams of the nearbed mean current flow indicate a component of cross-shelf directed flow, suggesting an enhanced potential for artifact preservation via cross-shelf advection of anoxic bottom waters by the near-inertial flows measured in this study.

BACKGROUND

The Black Sea provides an ideal natural laboratory for testing the role of shelf transport processes on bedform and artifact interaction (Özsoy and Ünlüata, 1997; Neretin et al., 2001; Coleman and Ballard 2004). This unique setting presents opportunities to test concepts of artifact-related scour and transport associated with complex sorted bedform features (Murray and Thieler, 2004; Trembanis et al., 2004; Green et al., 2004) and shipwreck artifacts (McNinch et al., 2006). The widespread occurrence and previous documentation of large-scale bedforms on the continental shelf (Ryan et al., 1997; Coleman and Ballard 2004; Lericolais et al., 2006) raises the question of whether these bedforms are (1) strictly modern; (2) ancient relicts; or (3) palimpsest features (i.e., relict but reworked) features. The objective of this study is to examine how the hydrodynamics (mean currents) of the shelf interact with the seafloor morphology over spatial scales ranging from meters to kilometers in a morphodynamic context similar to that used in other shelf studies (e.g., Trembanis et al., 2004; McNinch et al., 2006).

In addition to analyzing the distribution of bedforms (size and orientation), a secondary goal of this study is to relate the shelf hydrodynamic processes (internal waves) and seafloor morphology (bedforms) as important causative factors in shipwreck site and artifact preservation sensu (McNinch et al., 2006) with application to recent marine archaeological expeditions in the region (Coleman and Ballard, 2004). It has been hypothesized (Ryan et al., 1997; Coleman and Ballard, 2004) that interfacial internal waves assist in transporting anoxic waters onto and across the shelf providing a mechanism for enhanced artifact preservation above the normal oxycline. At the center of these hypotheses is the interplay between hydrodynamics and bed roughness. Previous observations (Ryan et al., 1997; Coleman and Ballard, 2004; Lericolais et al., 2006) suggest that there are strong analogs between the Black Sea shelf settings and the ubiquitous shelf sand body features originally termed "Rippled Scour Depressions" (Cacchione et al., 1984) that have been termed "Sorted Bedforms" in recent years (Murray and Thieler 2004; Trembanis et al., 2004). Of particular parallelism was the finding in New Zealand (Hume et al., 2003; Trembanis et al., 2004) that anoxic organic material in the sediment may have played a stabilizing role in controlling the lateral stability of the bedform features. It is possible that such deposits exist in the vicinity of the wreck sites in the Black Sea and perhaps these shear resistant deposits play a similarly important role in artifact and site preservation, whereby reduced organic layers might cap and help preserve the artifacts.

SHELF MORPHODYNAMICS

Field observations and theoretical refinements by numerous investigators over the past several decades have significantly advanced our understanding of shelf sediment transport processes (Thieler et al., 1995; Wright, 1995; Grant and Madsen, 1986). The continental shelf is an important transition region for physical, biological, and geological processes—one that forms a critical link between the nearshore and the deep-sea basin. The shelf is a morphodynamic system influenced by coupled physical, geological, chemical, and biological processes (Wright, 1995). Processes and phenomena of the shelf exhibit strong spatial and temporal variability, making this a complex four-dimensional region of study (Wright, 1995). Within this relatively shallow setting, frictional forces are important in connecting hydrodynamics to the behavior of seabed forms of varying scale (Grant and Madsen, 1986). In a strongly bidirectional manner, the bottom boundary layer structure depends heavily on the morphology of the seabed that in turn is shaped by gradients in the hydrodynamics (Wright, 1995). Furthermore, numerous studies of shelf settings around the world (Trembanis et al., 2004; Schwab et al., 2000; Drake, 1999; Wright et al., 1999; Riggs et al., 1998; Thieler et al., 1995; Cacchione and Drake, 1990) have documented that complexity is more the norm than the exception.

RIPPLES AND BEDFORMS

Ripples and other large bedforms on the shelf (e.g., sandwaves and subaqueous dunes) are important sources of seabed roughness to waves and currents (Ardhuin et al., 2002; Grant and Madsen, 1986) and play a key role in the nature and magnitude of sediment resuspension (Traykovski et al., 1999; Li et al., 1996; Cacchione and Drake, 1990). Several field and laboratory studies have been conducted in attempts to develop empirical formulae between ripple geometry (e.g., height, length, steepness) and flow conditions (Wiberg and Harris, 1994; Wikramanayake, 1993; Clifton and Dingler, 1984; Grant and Madsen, 1986; Nielsen, 1981; Miller and Komar, 1980). Under the typically irregular

flow conditions encountered in the field, the ability of these models to accurately predict observed ripple geometry has been shown to be rather poor (Trembanis and Traykovski, 2005; Trembanis et al., 2004; Doucette, and O'Donoghue 2002; Traykovski et al., 1999; Li et al., 1996; and Osborne and Vincent, 1993). In part, the reason for the poor agreement between field data and model estimates is that ripple geometries encountered in the field are often partially relict products of forcings from past events and not solely products of instantaneous hydrodynamic conditions. Both Traykovski et al. (1999) and Li and Amos (1999) observed significant hysteresis in ripple development on the shelf. In addition to non-equilibrium evolution, spatially varying grain size is another important issue affecting ripple dynamics (Green et al., 2004; Trembanis et al., 2004). Grain size and ripple dimensions on the shelf often exhibit large variations over spatial domains both greater than 1 km (e.g., Green et al., 2004; Hume et al., 2000; Black and Oldman, 1999; Barnhardt et al., 1998; and Field and Roy, 1984) and less than 1 km (e.g., Trembanis et al., 2004; Ardhuin et al., 2002; Thieler et al., 1995; Hunter et al., 1988; and Schwab and Molnia, 1987), often in correlation with sorted bedforms (previously termed "rippled scour depressions") that have wavelengths much longer than the ripples themselves (Green et al., 2004; Traykovski and Goff, 2003). According to Holland et al. (2003), heterogeneous patches of contrasting sediment grain size are frequently encountered along shelf environments around the world.

SCOUR

Scour is the morphodynamic response of the seabed as a result of the presence of an object or structure that disturbs the fluid flow (Soulsby, 1998). Scour is important for a variety of marine situations including bridge piers, dock pilings, breakwaters, oil platforms, offshore pipelines, marine artifacts, heterogeneous seabed bedforms, and naval mines (Whitehouse, 1998). The presence of an object on the seabed produces local flow acceleration due to continuity and thus drives a flux of local sediment and concomitant bed adjustments (Whitehouse, 1998). Another manifestation of scour is an increase in bed shear stress and turbulence as structured vortices are generated and released from around the object (Trembanis et al., 2007; McNinch et al., 2006).

Scour can be classified both in terms of spatial extent and hydrodynamics. Three spatial classes of scour are defined as: "local scour" which is in the immediate vicinity of the object (on the order of meters), "global scour" composed of wide depressions around large or multiple objects (on the order of 10s of meters), and "overall seabed movement" associated with large scale (100s–1000s of meters) patterns of erosion, deposition, and bedform movement (Whitehouse, 1998). In terms of hydrodynamic intensity, scour is classified as either clear-water, when the ambient flow (bed shear stress) is below threshold velocity, or live-bed, when ambient flow is above threshold velocity and the entire bed is active. In the former, the amplification of flow about the object induces transport locally but elsewhere the bed is immobile. In the latter case, sediment is being transported by flow everywhere, but especially near the object, where turbulence and bed shear stress are enhanced (Trembanis et al., 2007; McNinch et al., 2006).

Once an object is exposed on the seabed, scour is initiated around the lateral ends of the object because of converging accelerated flow. This convergence leads to progressive erosion of the sediment from under the ends of the object, forming an expanding scour pit and shrinking the support pedestal. The object then will settle into its scour pit in a series of rocking and rolling motions until it is no longer protruding above the ambient seabed or until flow conditions subside and backfilling (deposition) ensues (see McNinch et al., 2006, and figures therein). In non-steady flows, periods of excavation (scour) will normally be interrupted by episodes of backfilling (deposition) (Trembanis et al., 2007; Richardson and Traykovski, 2002; Fredsoe, 1978). A possible sequence for scour around a free settling horizontal object, such as those examined in this study, is illustrated in McNinch et al. (2006; their fig. 4).

HYDRODYNAMICS AND BEDFORMS

Like no other large body of water in the world, the Black Sea (Fig. 1) has an upper oxygenated layer and a lower anoxic layer. The interface between the layers reaches down to 180 m depth along the coastal margins, and 500 m near the Bosporus (Özsoy and Ünlüata, 1997; Neretin et al., 2001). This interface appears to be unstable and at varying times, probably during severe weather conditions, creates internal waves that break upon the Black Sea's continental shelf along the oxic/anoxic boundary. The surface layer in the Black Sea averages 18‰ salinity and 22 °C, and is highly oxygenated. The surface circulation features a cyclonic rim current about the entire basin. Two cyclonic gyres occur within the outer rim current, as well as eddies and intermittent convection to intermediate depths by surface cooling. The transition from the surface to the denser, trapped deep layer is marked by an oxycline with steep gradients in salinity, temperature, and chemical content. The deep-water averages 22‰ salinity and 8 °C and is completely anoxic while being rich in hydrogen sulfide (H_2S) and ammonium (Özsoy and Ünlüata, 1997). The density contrast between these layers is large enough to support the propagation of internal waves. Internal waves with periods of six minutes and more, and with bottom velocities on the order of 30 cm/s, fast enough to exhume and carry suspended silt and fine sand (Hjulström, 1935; Prothero and Schwab, 2004), have been observed on the southern coast of Crimea (Filonov, 2000). When the crest of such a wave meets the continental shelf like that of the Danube delta in the northwest, the anoxic, H_2S-rich water runs up and down the slope in a manner precisely analogous to the swash and backswash of a surface wave on a beach—whether in linear or turbulent fashion—and almost certainly has a large effect on the benthic environment. The anoxia and high H_2S content of the wave water would kill most or all organisms it

contacts. In certain areas bottom topography may contribute to a rapid enough backswash to cause sediment entrainment, erosion, and the development of bedforms (McPhee-Shaw, 2006).

Internal waves have two important geoarchaeological effects. The first is the creation of a mixed layer between 85 and 185 m that periodically leads to anoxic water conditions. These anoxic water conditions are of interest to archaeologists since they lead to the long-term preservation of ancient wooden shipwrecks (Coleman and Ballard, 2004). The second is the creation of bedforms characterized by large sand waves that lay in a depth zone of 85–185 m. These bedforms are of interest because:

- the existence of these shelf-sorted bedform features is poorly documented and not well understood;
- the hydrodynamics responsible for these bedforms may help transport anoxic water across the shelf; and
- the introduction of anoxic water onto the continental shelf by internal waves may preserve ancient wooden shipwrecks at far shallower depths than previously thought.

FIELD SITE AND RESEARCH METHODS

The field site was located off the southwest coast of the Crimean Peninsula of the Northern Black Sea (Fig. 1). In 2006, a geoacoustical survey was conducted of the southwestern Crimean shelf and slope (Fig. 2) along a suspected deep-sea trade route between the Bosporus and the Crimea. A number of side-scan sonar targets were identified that were later inspected with a remotely operated vehicle. Several of the targets turned out to be modern shipwrecks and aircraft (mostly Russian from the Crimean War, World War I, and World War II eras), but one of the targets, located ~23 km off the coast, was a pile of ancient ceramic jars. Based on the typology of similar-looking jars from the Chersonesos site (Ryzhov and Sedikova, 1999) and elsewhere around the Black Sea region (e.g., Hayes, 1992), these jar types are estimated to date between the ninth and eleventh centuries C.E., placing the ship in the early Medieval Period. At a depth of ~150 m, this shipwreck lies above the normal anoxic interface but within the mixed layer of temporally varying dissolved oxygen content. It has thus escaped the ravages of marine borers and appears to be in an unusually good state of preservation. In general, this mixed layer is prevalent throughout the entire Black Sea basin along the shelf break between depths of ~80–180 m (Ballard et al., 2001). The side-scan sonar data collected in 2006 forms the basis of the large-scale bedform mapping presented in this paper (Figs. 2 and 3).

Figure 1. Study-site location map (star) off the SW coast of the Crimean peninsula at a local depth of ~135 m. Inset illustrating the side-scan sonar surveys in the vicinity of the bottom mooring associated with the shipwreck site known as *Chersonesos A* (star).

SENSOR CONFIGURATION AND SAMPLING REGIME

In addition to the side-scan sonar surveys conducted in 2006 (Figs. 2 and 3), a set of bottom-mounted instruments (Fig. 4) were deployed in 2007 measuring currents, temperature, salinity, and seabed geometry. The bottom-mount (Fig. 4A) was located at a depth of 135 m and included an upward-looking acoustic Doppler current profiler (ADCP), conductivity-temperature (CT) logger, and rotary fanbeam sonar. The CT sensor provides a time-series point measurement of the ambient salinity and temperature used to determine changes to the density of the surrounding water and the passage of thermocline or pycnocline oscillations (Fig. 6). The ADCP gathers vertical profiles of three-dimensional hydrodynamic flow (Fig. 7) recorded in earth-coordinates (i.e., east-west, north-south, up-down) based on an internal compass. The rotary fanbeam sonar (Fig. 4B) obtains a high-resolution planview image of the seabed surrounding the bottom mount to a range of 9 m thus providing a time-lapse picture (Fig. 5) of the small-scale bedform geometry and dynamics in for comparison to the hydrodynamic measurements. Table 1 summarizes the sampling scheme settings for each of the bottom-mount instruments.

On 15 August 2007, the ADCP/CT/Sonar bottom mount was deployed in the vicinity of the *Chersonesos A* wrecksite at a local depth of 135 m and was recovered after ~38 h. Upon recovery, data was downloaded and archived. The data analysis results are presented below.

RESULTS AND DISCUSSION

Salinity and Temperature Record

Figure 6 illustrates the recorded time series of temperature (blue line) in °C and salinity (green line) in ‰ at a height of 0.75 m above the bed. The Sea-Bird SBE-37SM sensor recorded every 23 seconds, the fastest sampling scheme that would cover the expected deployment duration. The sharp drop in temperature

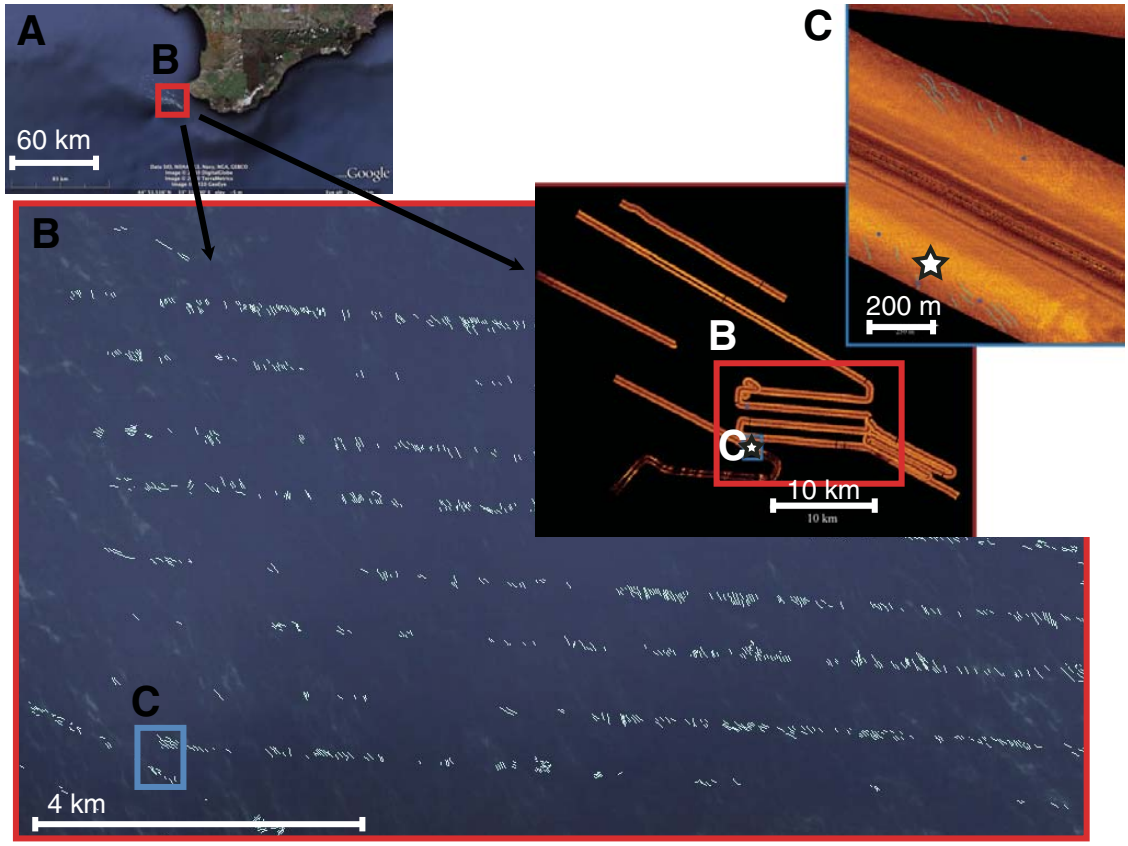

Figure 2. Map plot illustrating several hundred of the more than 2300 bedforms digitized in geographic information systems. The crest line of each visible bedform was digitized from the side-scan sonar survey data. Insets are as follows: (A) Cape Sarych and the surrounding vicinity; (B) Digitized bedform crests in a 10 km box surrounding the *Chersonesos A* wreck site; (C) Close-up portion of the survey site showing digitized bedforms (blue lines) over the side-scan sonar record. Star illustrates location of the acoustic Doppler current profiler/conductivity-temperature sensor/Rotary sonar bottom mooring.

and rise in salinity at the beginning of the deployment represents the measurements as the instrument mount was descending through the water column during deployment. A reverse signal is seen at the end of the deployment when the bottom mount was recovered from the seabed. During the interval between descent and recovery, the CT sensor recorded essentially static values for salinity and temperature. The mean temperature was 8.3 °C with a standard deviation of 0.03 °C. Mean salinity was 20.6‰ with a standard deviation of 0.08‰. The slight changes in the values during the deployment and the sharp changes at the beginning and the end confirm that the sensor was in fact working and that the nearly flat line plots of temperature and salinity were in fact real. We initially expected sharp fluctuations in temperature and salinity coinciding with the interface of the pycnocline oscillating about the depths of the deployment site with a high-frequency interval, which might have come from internal waves breaking across the shelf. The absence of these high-frequency oscillations in our data does not imply that these waves do not exist but simply that we did not observe them during our short deployment, which was conducted during fair-weather conditions rather than a storm period when internal waves would most likely occur. Salinity and temperature measurements illustrate the general background conditions for this site. If our measurements are well and truly above or below the pycnocline, it could be that the signature of the internal waves (if present) are not reflected in the temperature and salinity signals but rather in the mean current flow, examined in the next section.

Current Structure and Velocity Time-Series

The key critical observations of mean current structure and time-series behavior are illustrated in Figures 7 and 8. The 300 kHz ADCP used in this study was set to the smallest vertical bin size (2 m) and a rapid profile repeat rate (30 second interval) in order to maximize the vertical and temporal resolution of the measurements with hopes of encountering high-frequency internal waves. Each 30-second burst represents an ensemble average of 16 individual acoustic pings over a vertical range from 4.2 m

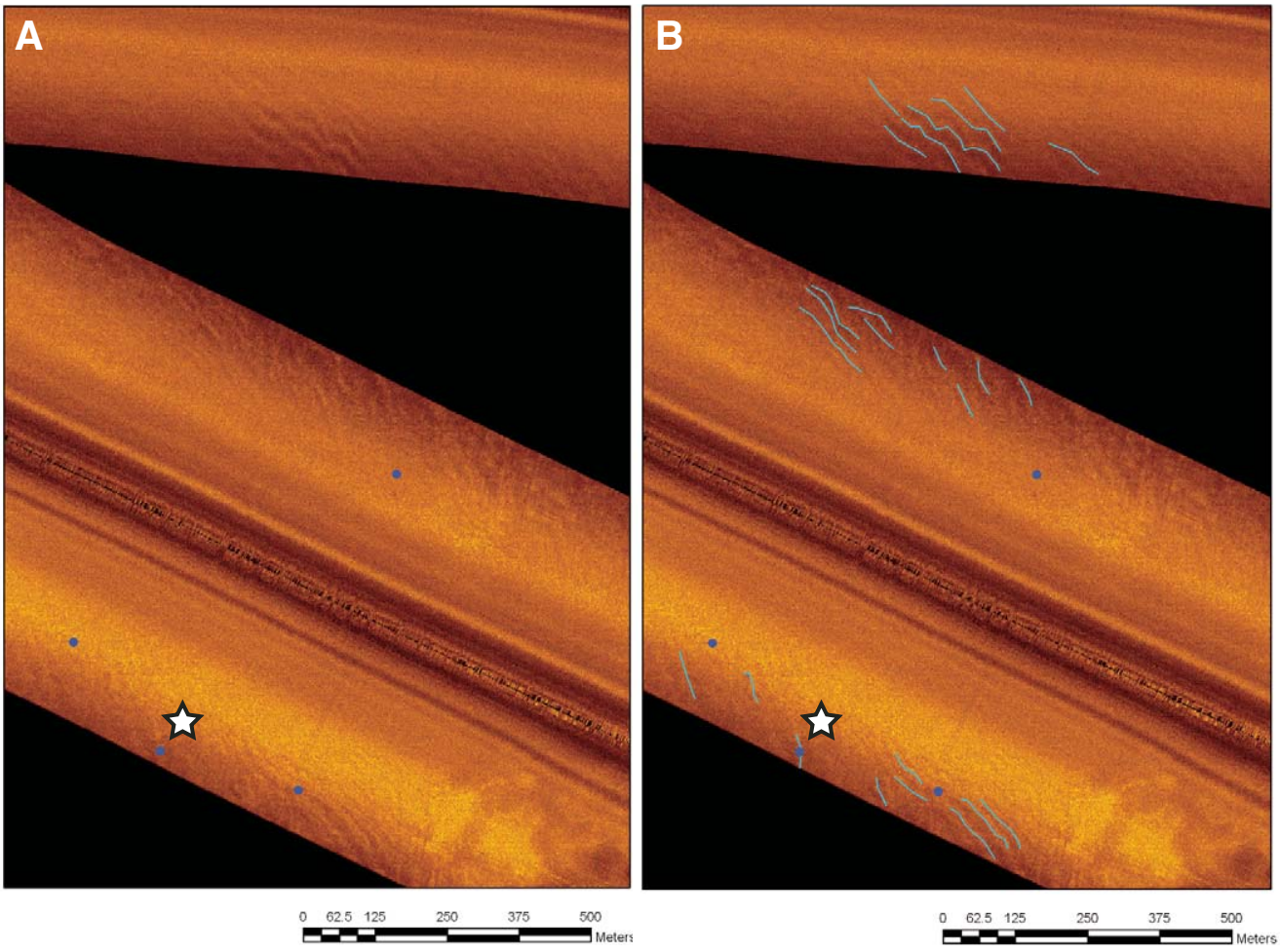

Figure 3. Side-by side comparison of side-scan sonar record showing raw georeference image (A) and geographic information system digitized bedforms (B). Star illustrates location of the acoustic Doppler current profiler/conductivity-temperature sensor /Rotary sonar bottom mooring.

above the bed to over 80 m above the bed, with horizontal and vertical measurements occurring every 2 m. A resulting color contour plot of the magnitude of the velocity (i.e., speed) of the horizontal current component, i.e., the Pythagorean addition of the east-west and north-south components of the flow, is illustrated in Figure 7. While a great deal of vertical and temporal structure exists in this figure, we will limit our discussion of the current velocity structure near to the bed (<10–20 m) especially the lowest bin at a height of 4.2 m above the bed, because the nearbed flows have the greatest influence on sediment transport and the formation of bedforms run-on. The lowest bin height is a function of the fundamental frequency of the ADCP (300 kHz), and the blanking distance beyond which valid velocity samples are returned. Of particular note are the two pulses of higher velocity near-bed flow that begin at ~5 h and 20 h respectively after the start of the deployment (Fig. 7). Each pulse episode lasts between 6 and 8 h with velocities ranging from 15 to 25 cm/s. The vertical structure during each pulse episode exhibits a general upsweep pattern in space and time with the highest velocities being recorded at the lower bins and decreasing away from the bottom up into the water column rising to as much as 30 m above the bed. Above this lower pulse layer is a zone 30–50 m above the bed where the speed drops to values of around 5 cm/s. This pattern suggests a velocity source from a lateral area moving across the mooring site and not a source from surface derived current (Fig. 7).

Further insights into the local flow dynamics can be obtained by examining the time series of the lowermost bin. In Figure 8, the individual vector component time-series are portrayed for the bin 4.2 m above the bed. Here, several flow trends are evident. First, there is a deployment averaged net vector in the U component of 10 cm/s to the west and in the V component of 0.34 cm/s to the north. Overall, the current follows a progressive anticyclonic path generally following the shelf break toward the west with pulses toward the north-northwest. The two pulses toward the north-northwest are illustrated by the sharp bumps in the V component of the horizontal flow, with peaks in excess of 10 cm/s to the north (Fig. 8).

The most important flows for sediment transport purposes are those with a competence (intensity) sufficient to initiate or

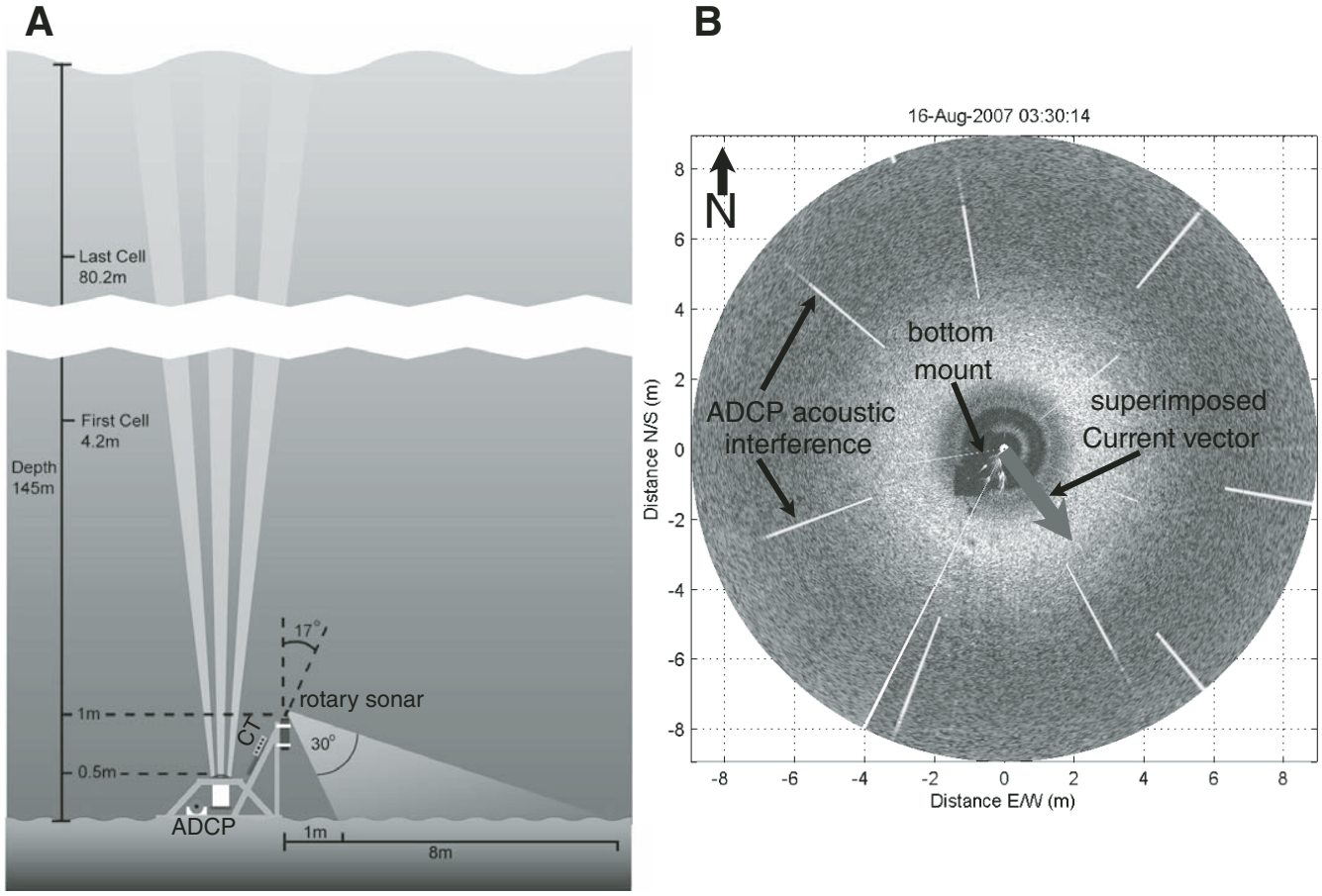

Figure 4. (A) Schematic illustrating the configuration of the seabed mooring composed of acoustic Doppler current profiler (ADCP), conductivity-temperature sensor (CT) and rotary fanbeam sonar. (B) Rotary fanbeam sonar single pass scan image collected from the seabed mooring in the vicinity of the *Chersonesos A* site. High intensity backscatter returns are light pixels, while dark pixels are low backscatter.

maintain the transport of sediment, in this case flows above the mean velocity of 12.45 cm/s. Based on the classic Hjulström curve (Hjulström, 1935) the mean flow (12.45 cm/s) encountered at the field site (Fig. 8) implies that the very fine to medium sands will remain in transport while the coarse sands and gravels exposed in the lower shell-hash/gravel facies will remain as un-entrained deposits. During peak observed flows (20 cm/s), the erosion threshold for the very fine and fine sands is met suggesting that fine/very-fine sands will be exhumed from the seabed exposing previously buried coarse sand/gravel shell hash units. This process of feedback between flow and scour sorting was previously documented in the work of Trembanis et al., (2004) and Green et al., (2004) for other shelf settings and suggests a similar set of processes are at work on the outer shelf of the Northern Black Sea.

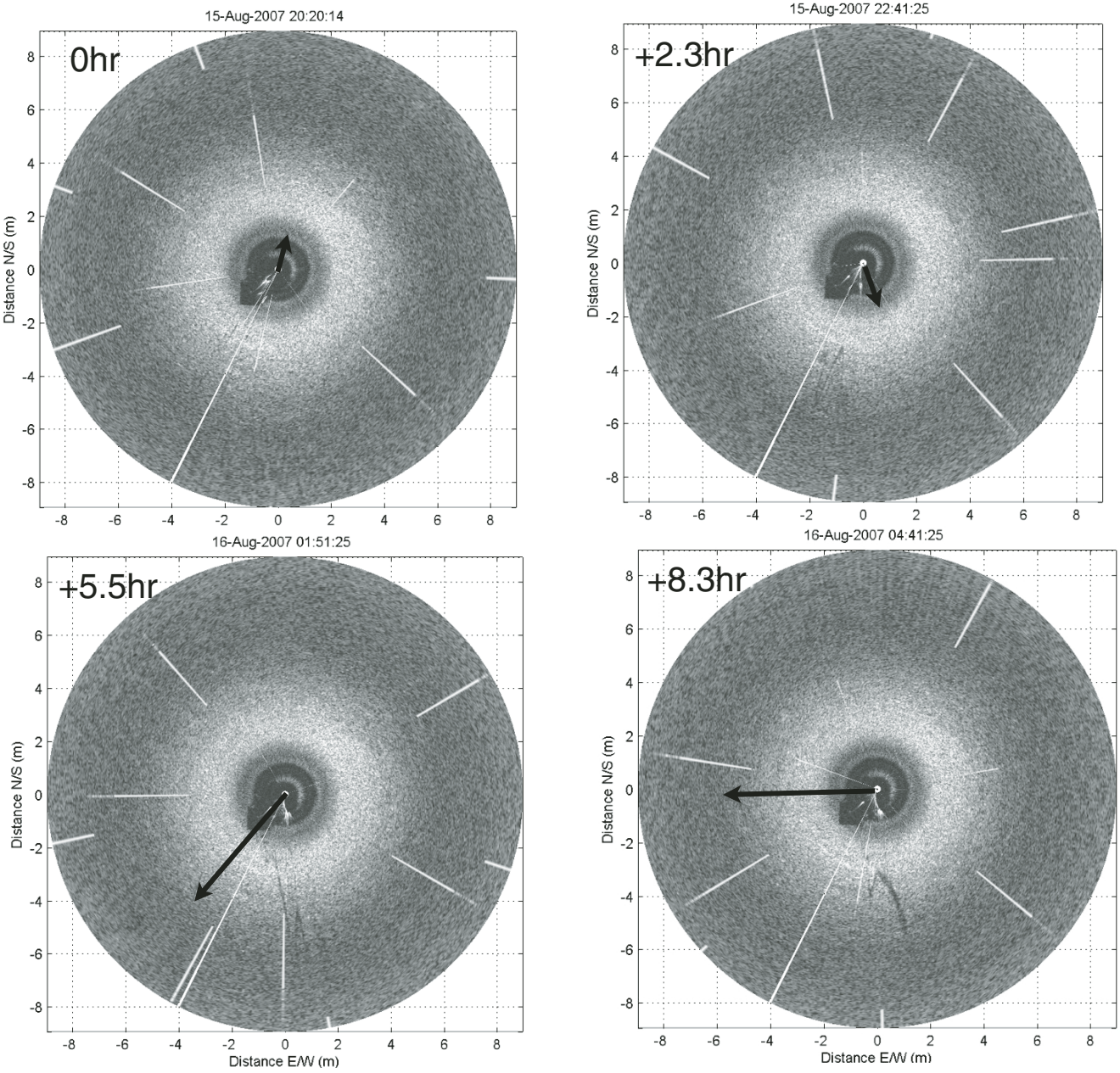

Figure 5. Time-lapse images of rotary sonar scans over an 8 h period together with overlay of the mean current vector at the time of the scan (arrow). The time progression shows subtle ripples toward the outer ranges of the sonar scan but otherwise stasis in the bed configuration over this short time period. The current vectors illustrate a progressive anticyclonic mean current pattern with currents strengthening toward the S/SW.

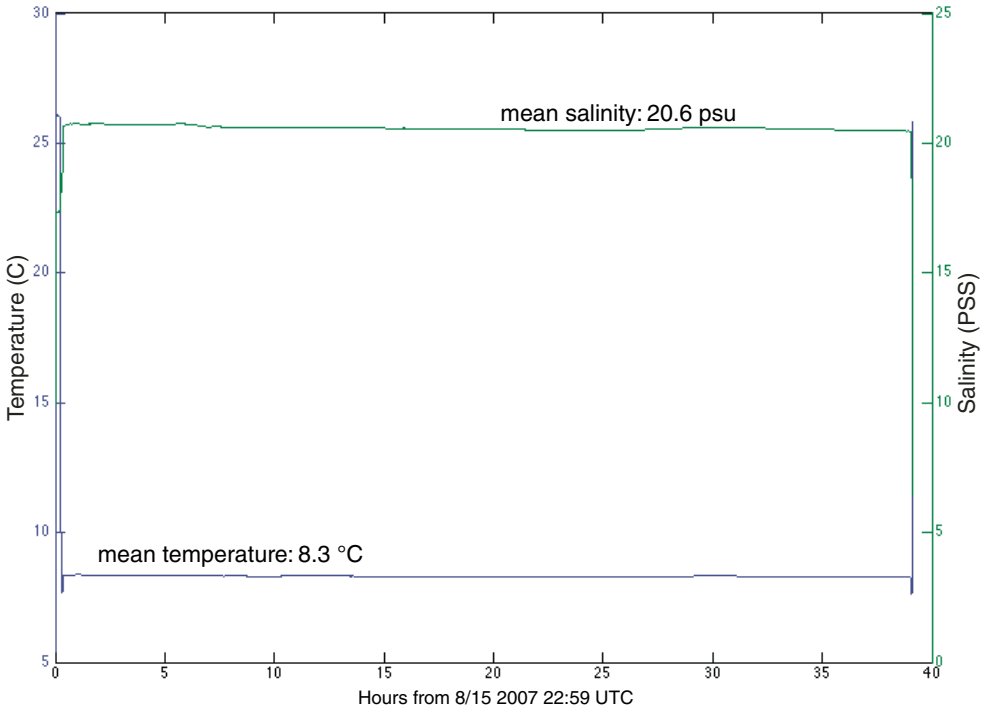

Figure 6. Time-series plot of temperature (blue) and salinity (green) as recorded every 23 seconds by the conductivity-temperature sensor on the bottom mooring.

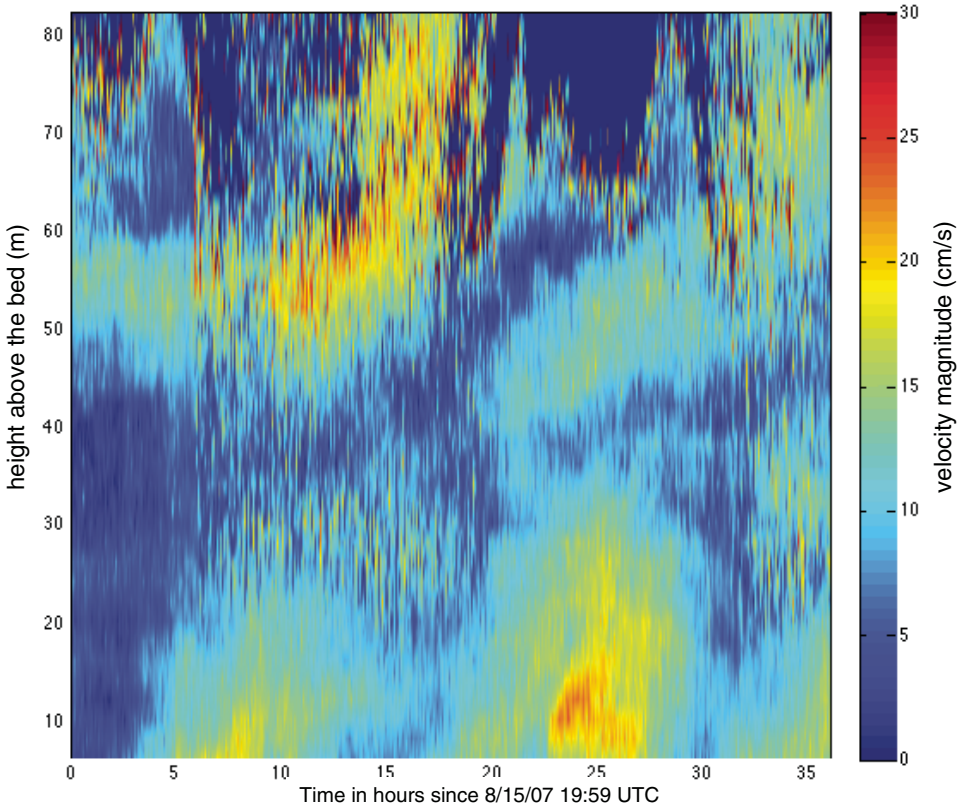

Figure 7. Vertical cross-section color-contour plot of horizontal current speed (magnitude of velocity) measured between 4.2 and 84 m above the seabed in a local depth of 135 m. Bin 1 is located 4.2 m above the bed.

TABLE 1. INSTRUMENT SAMPLING CONFIGURATION SUMMARY

Instrument	Phenomenon	Depth (m)	No. of data points	Sampling interval	Sampling rate
Side-scan sonar Datasonics SIS-1000, 100 kHz, 200 m range, May 2006	Digitized bedforms over entire shelf	113–237	2376	1 survey	1 survey
TRDI ADCP, 300 kHz, 2 m bins, August 2007	Mean currents; transport processes	4.2–80 m above bed	11,021	30 s	1 burst with 16 pings
Imagenex 881-tilthead Rotary Sonar, 2.25 MHz, 9 m range, August 2007	Ripple geometry/evolution	135 (1 m above bed)	292	10 min	3 scans
SBE-37SM, August 2007	Salinity; temperature	135 (0.75 m above bed)	6124	23 s	1 burst

Energetic Near-Inertial Coastal-Trapped Waves

The upper layer waters of the Black Sea are characterized by a predominantly cyclonic, rim current flowing along and occasionally across the continental shelf in a strongly variable spatiotemporal pattern. In addition, a series of quasi-permanent anticyclonic eddies exist inshore of the rim current (Oguz et al., 2005). The rim current structure is accompanied by coastal-trapped waves (CTWs) with an embedded train of eddies and meanders propagating cyclonically around the basin (Oguz and Besiktepe, 1999). According to the ADCP measurements (Oguz and Besiktepe, 1999), the rim current jet has a speed of 50–100 cm/s within the upper layer, and ~10–20 cm/s within the 150–300 m depth range. These shelf current features provide a mechanism for bidirectional transport between the nearshore and offshore regions. The most notable features of the Black Sea circulation system in relation to this study include (*i*) the meandering rim current system cyclonically encircling the basin and (*ii*) the Crimea and Sevastopol anticyclonic eddies on the coastal side of the rim current zone. It is important to note that the observations in this study were taken near the junction of the rim current and the Sevastopol anticyclonic eddy, termed a

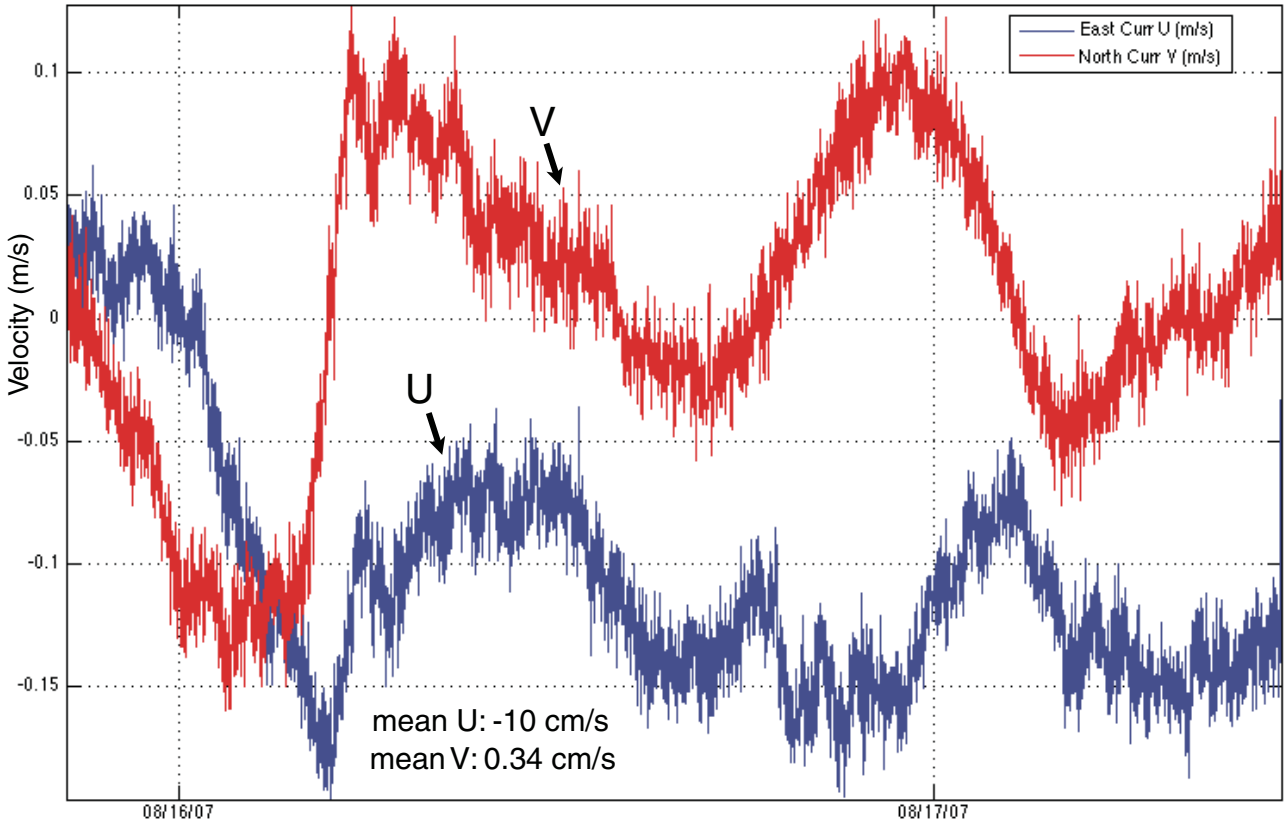

Figure 8. Time-series plots of horizontal components of mean current measured every 30 seconds at bin 1 (4.2 m above the bed). Red line shows north-south flow (north positive) and the blue line represents east-west flow (east positive).

"quasi-permanent or recurrent feature" in the upper layer circulation by Oguz et al. (2005).

Because of strong stratification in the Black Sea, CTWs reach the inertial frequency. Furthermore, their velocity fluctuations are surface-intensified off the shelf break (over the upper slope), but reverse to bottom-intensified on the shelf (Ivanov and Yankovsky, 1993). The velocity amplitude of CTWs on the South Crimean shelf is ~10–15 cm/s in the summer and is likely to be higher during the winter season notorious for its severe storms. CTWs propagate with the coast on the right (as a Kelvin wave), westward in the Northern Black Sea. As CTWs encounter coastline and topographic variations past Cape Sarych (the southernmost tip of the Crimea Peninsula) they scatter into other (higher) wave modes in order to adjust to these "disturbances" of the waveguide. Scattering typically introduces smaller spatial scales and higher amplitudes in the wave field. Indeed, the outer shelf and slope just to the west of Crimea, in the vicinity of our deployment site (star in Figs. 1–3), is characterized by strong mesoscale variability with frequent predominantly anticyclonic eddies. This particular feature of the regional shelf dynamics prompted a series of papers aimed at examining the phenomenon (i.e., Yankovsky and Chapman, 1995, 1996, 1997). In these papers, the authors found that very energetic vortex-like current patterns could be developed in the near bottom layer with near-inertial or subinertial frequencies.

In addition to the CTWs, the rim current itself meanders and makes episodic onshore excursions. An example of this behavior can be found in the vertical transect of the rim current by Oguz and Besiktepe (1999; their fig. 3). The implications of these processes (CTWs, meanders in the rim current, and potential storm-induced internal waves) is that there are a number of physical processes that can promote cross-shelf transport (including anoxic waters) across the shelf and contribute to the scour and preservation potential in the region.

Bedform Distribution and Scour Patterns

During the 2006 field campaign, over 300 km of linear survey line was run with the 100 kHz side-scan sonar towfish. Each survey line was processed for water-column removal, layback positioning, and beam angle correction using the SonarWiz™ (Chesapeake Technology Inc.) processing system to generate a final georeferenced sonar mosaic as illustrated in Figure 2 (inset). Next, each line was examined and all discernable bedforms were digitized (Fig. 3) using the heads up GIS feature of SonarWiz. In total, 2376 individual bedforms were digitized in this manner providing a GIS data set for subsequent analysis. Both the side-scan sonar mosaic and the digitized bedforms were exported to the Google Earth™ KML file format to allow viewing and wider distribution of the results (Figs. 2 and 3). Once digitized, wavelength spacing between each successive bedform was calculated from the centroid of each bedform to the next, with a resulting mean and modal wavelength calculation of 72.8 and 15.7 m respectively (Fig. 9A). Furthermore, for each bedform, a corresponding strike orientation (along-crest) and dip (crest orthogonal) orientation was determined (Fig. 9B). Recall that azimuth and dip are orthogonal, therefore, the principal dip orientation as determined from least squares rotation analysis was found to be 52°/232° (Fig. 9B). The 180° ambiguities in bedform dip direction (52°/232°) are a result of the two-dimensional nature of side-scan sonar data and the lack of bathymetric data to determine the stoss (updrift) face from the lee (downdrift) face of the bedform. In Figure 9C, a comparison between the bedform dip orientation (blue dots) and the nearbed mean current (velocity amplitude of 12–20 cm/s) displayed a close association with peak flows (red arrows) in a crest-orthogonal direction. It seems most likely given the observed flow regime that the direction of lee face is 232°.

A progressive vector diagram of the nearbed current (Fig. 10) also shows the connection between bedform orientation and shelf transport flows. Assuming an idealized homogeneous lateral flow regime, the progressive vector diagram illustrates the path that a particle of water near the bed would take over the period of the bottom mount deployment. This shows the general westerly flow with several turns to the north-northwest associated with the strong pulses of nearbed flow, further emphasizing that adiabathic flows do commonly occur in this region.

SUMMARY AND CONCLUSIONS

The Northern Black Sea shelf is a complex, heterogeneous, morphodynamic system that provides a critical link between the nearshore and the deep sea (Fig. 1). Marked spatial and temporal variations in bedform geometry as well as sharp gradients in forcing conditions (rim current, CTWs) typify the shelf setting. Increasing our present understanding of the coupled links between variable bed geometry and hydrodynamics is a crucial step in order to decipher the morphologic history of the Black Sea shelf since the end of the Last Glacial Maximum.

In this study, we found no appreciable variation in nearbed salinity or temperature during the deployment of our instrumented bottom mount, suggesting absence of baroclinic driven flows during this period (Fig. 5). Furthermore, the ADCP measurements of nearbed flows also gave no indication of high-frequency internal wave activity during the deployment, suggesting that these events may be highly seasonal and event driven. Nevertheless, significant and distinct nearbed flow features were observed during the field deployment as evidenced by the observed quasi-steady, near-inertial flows that were decoupled from surface and showed strongest velocities near the bed (Figs. 6 and 7). The currents, possibly CTWs oscillated with ~15 h periodicity and amplitude of ~15 cm/s. Previous physical oceanographic work in the region suggests that there are several reasons to expect strong variations of near bottom currents in the near-inertial–subinertial frequency range on the outer shelf southwest of Sevastopol including CTWs and meanders in the rim current.

This study presents a new observational investigation of bedform distribution and the relation of bedform geometry to

nearbed hydrodynamics (Fig. 8C). Previously suggested theories suggest that these bedforms are static ancient features, a theory that is perhaps correct only for isolated instances. The observed flow dynamics and bedform orientations imply an increased preservation potential of artifacts on the shelf. Furthermore, the observed outer shelf flows (Fig. 10) may also reduce the depth of viable preservation in artifacts that would otherwise exist above the anoxic layer. The occurrence of presently active bedforms on the outer shelf as documented here, further emphasizes the role that CTWs, internal waves, and rim currents have on the transport of water and sediment across the shelf.

ACKNOWLEDGMENTS

The authors wish to acknowledge the financial and technical support of the following groups: the officers and crew of the NRV *Alliance*, the office of the President of Ukraine, U.S. National Oceanic and Atmospheric Administration (NOAA) Office of Ocean Exploration and Research, the Office of Naval Research, the Center for Coastal and Ocean Mapping at the University of New Hampshire, and the National Geographic Society. The authors particularly thank Drs. Tony Rodriguez and Doug Levin for reviews that substantially improved the paper.

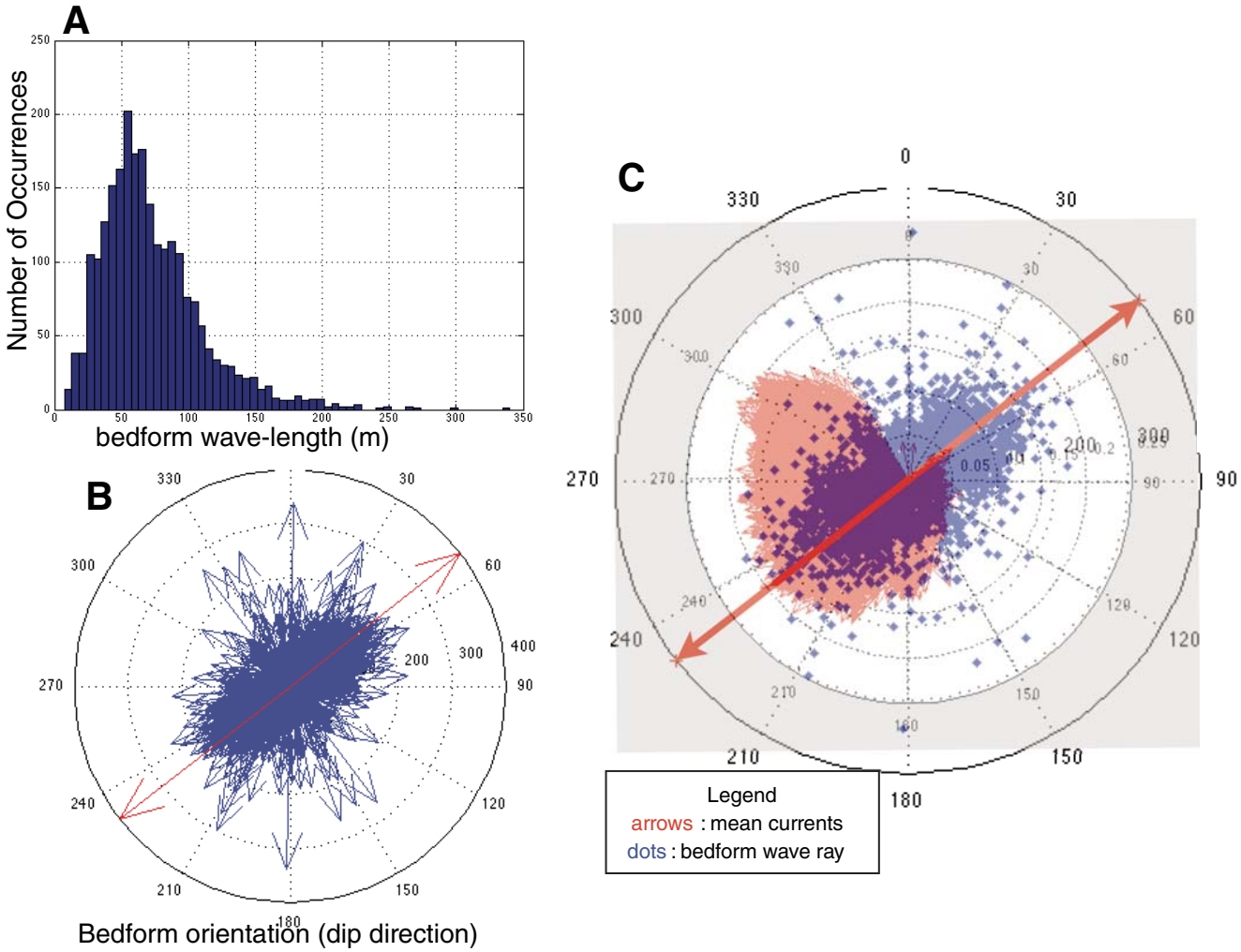

Figure 9. (A) Histogram of bedform wavelength (e.g., spacing between crests) for each of the bedform pairs in the digitized record. N = 2376 and mean wavelength 72.8 m (B) Compass plot of bedform of dip azimuth (orthogonal to crest), calculated from the geographic information system digitized side-scan sonar. N = 2376 and principle dip azimuth of 52/232 degrees true north. Crest orthogonal azimuth has a 180° ambiguity depending on which side of the bedform is used for the origin reference, therefore the conjugate pair for each crest orthogonal is shown (blue arrows) and the principle bedform orientation is shown by the long red arrow. (C) Mean currents (red arrows) overlain on bedform wave ray (blue dots). Principle bedform dip orientation, determined by least squares rotation analysis, is shown by the thick red arrow. Note: Currents are in the direction of propagation and bedforms are shown as conjugate direction across crest.

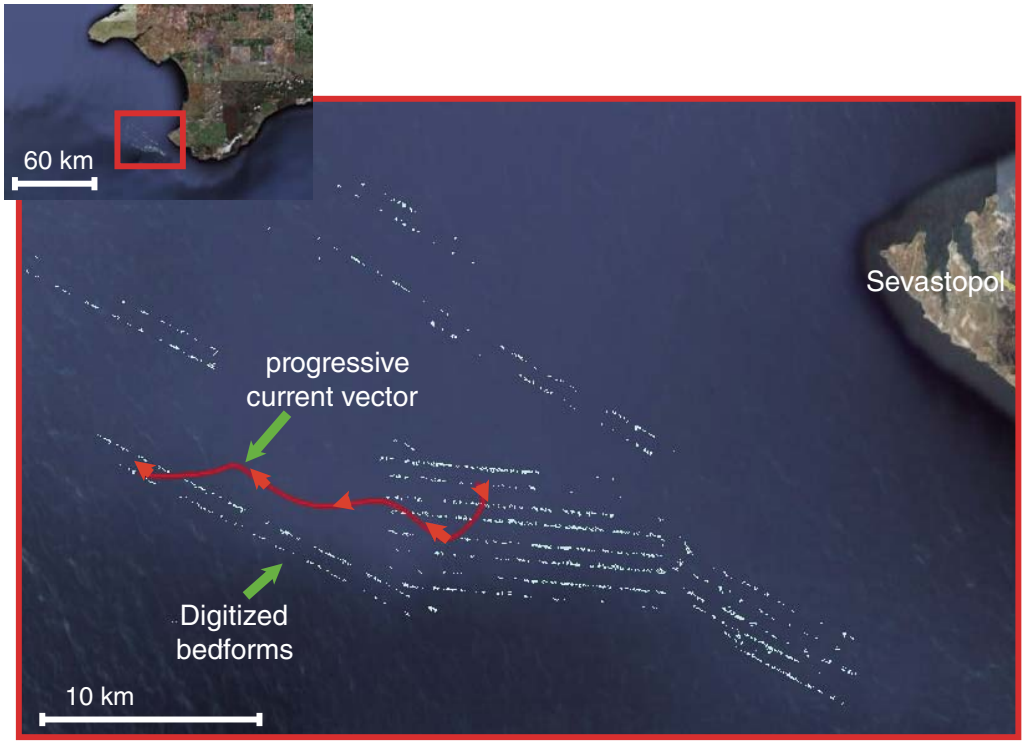

Figure 10. Progressive vector diagram plot of bottom acoustic Doppler current profiler bin mean current illustrating net current transport near the bed.

REFERENCES CITED

Ardhuin, F., Drake, T.G., and Herbers, T.H.C., 2002, Observations of wave generated vortex ripples on the North Carolina continental shelf: Journal of Geophysical Research, v. 107, no. C10, p. 7-1–7-14.

Ballard, R.D., Hiebert, F.T., Coleman, D.F., Ward, C., Smith, J., Willis, K., Foley, B., Croff, K., Major, C., and Torre, F., 2001, Deepwater archaeology of the Black Sea, 2000 season at Sinop, Turkey: American Journal of Archaeology, v. 105, no. 4, p. 607–623, doi:10.2307/507409.

Barnhardt, W.A., Kelley, J.T., Dickson, S.M., and Belknap, D.F., 1998, Mapping the Gulf of Maine with side-scan sonar: a new bottom type classification for complex sea floors: Journal of Coastal Research, v. 14, p. 646–659.

Black, K.P., and Oldman, J.W., 1999, Wave mechanisms responsible for grain sorting and non-uniform ripple distribution across two moderate-energy, sandy continental shelves: Marine Geology, v. 162, p. 121–132, doi:10.1016/S0025-3227(99)00060-2.

Cacchione, D.A., and Drake, D.E., 1990, Shelf sediment transport: An overview with applications to the Northern California Continental Shelf, *in* LeMehaute, B., and Hanes, D., eds., The Sea: New York, John Wiley and Sons, Ocean Engineering Science, v. 9, part B, p. 729–773.

Cacchione, D.A., Drake, D.D., Grant, W.D., and Tate, G.B., 1984, Rippled scour depressions on the inner continental shelf off Central California: Journal of Sedimentary Petrology, v. 54, p. 1280–1291.

Clifton, H.E., and Dingler, J.R., 1984, Wave-formed sedimentary structures and paleoenvironmental reconstruction: Marine Geology, v. 60, p. 165–198, doi:10.1016/0025-3227(84)90149-X.

Coleman, D.F., and Ballard, R.D., 2004, Archaeological oceanography of the Black Sea, *in* Akal, T., Ballard, R.D., and Bass, G.F., eds., The Application of Recent Advances in Underwater Detection and Survey Techniques to Underwater Archaeology: Istanbul, Uluburun Publishing, p. 49–58.

Doucette, J.S., and O'Donoghue, T., 2002, Sand ripples in irregular and changing wave conditions: a review of laboratory and field studies: University of Aberdeen, Department of Engineering, European Commission Marine Science and Technology (EC MAST) Program, Project No. MAS3-CT97-0086, 18 p.

Drake, D.A., 1999, Temporal and spatial variability of the sediment grain-size distribution on the Eel shelf: the flood layer of 1995: Marine Geology, v. 154, p. 169–182, doi:10.1016/S0025-3227(98)00111-X.

Field, M.E., and Roy, P.S., 1984, Offshore transport and sand-body formation—Evidence from a steep, high-energy shoreface, Southeastern Australia: Journal of Sedimentary Petrology, v. 54, p. 1292–1302.

Filonov, A.E., 2000, Thermic structure and intense internal waves on the narrow continental shelf of the Black Sea: Journal of Marine Systems, v. 24, p. 27–40, doi:10.1016/S0924-7963(99)00077-9.

Fredsoe, J., 1978, Experiments of natural backfilling of pipeline trenches. Institute of Hydrodynamics and Hydraulic Engineering: Technical University of Denmark Program Report, v. 46, p. 3–6.

Grant, W.D., and Madsen, O.S., 1986, The continental shelf bottom boundary layer: Annual Review of Fluid Mechanics, v. 18, p. 265–305, doi:10.1146/annurev.fl.18.010186.001405.

Green, M.O., Vincent, C.E., and Trembanis, A.C., 2004, Suspension of coarse and fine sand on a wave-dominated shoreface, with implications for the development of rippled scour depressions: Continental Shelf Research, v. 24, p. 317–335, doi:10.1016/j.csr.2003.11.002.

Hayes, J.W., 1992, Excavations at Sarachane in Istanbul II: The Pottery: Princeton, New Jersey, Princeton University Press, p. 117, deposit 39, fig. 63.6 (mid tenth century); 122–23, deposit 42, fig. 68.41 (mid eleventh century); 124–26, deposit 43, fig. 71.53 (after middle of the eleventh century).

Hjulström, F., 1935, Studies of the morphological activity of rivers as illustrated by the river Fyris: Uppsala University, Geological Institute Bulletin 25, p. 221–527.

Holland, K.T., Keen, T.R., Kaihatu, J.M., and Calantoni, J., 2003, Understanding coastal dynamics in heterogeneous sedimentary environments, *in* Davis, R.A., Sallenger, A., and Howd, P., eds., Coastal Sediments '03, Crossing Disciplinary Boundaries: Proceedings of the 5th International Symposium on Coastal Engineering and Science of Coastal Sediment Processes, World Scientific Publishing, Hackensack, New Jersey, 6000 p.

Hume, T.M., Oldman, J., and Black, K.P., 2000, Sediment facies and pathways of sand transport about a large deep-water headland, Cape Rodney New Zealand: New Zealand Journal of Marine and Freshwater Research, v. 34, p. 695–717, doi:10.1080/00288330.2000.9516971.

Hume, T.M., Trembanis, A.C., Hill, A., Liefting, R., and Stephens, S., 2003, Spatially variable, temporally stable, sedimentary facies on an energetic inner shelf, *in* Davis, R.A., Sallenger, A., and Howd P., eds., Coastal Sediments '03, Crossing Disciplinary Boundaries: Proceedings of the 5th International Symposium on Coastal Engineering and Science of Coastal Sediment Processes, World Scientific Publishing, Hackensack, New Jersey, 6000 p.

Hunter, R.E., Dingler, J.R., Anima, R.J., and Richmond, B.M., 1988, Coarse-sediment bands on the inner shelf of Southern Monterey Bay, California: Marine Geology, v. 80, p. 81–98, doi:10.1016/0025-3227(88)90073-4.

Ivanov, V.A., and Yankovsky, A.E., 1993, Local dynamics experiment in the shelf zone of Southern Crimean coast: Okeanologiya, v. 33, p. 49–56.

Lericolais, G., Bulois, C., and Gillet, H., 2006. Coastal sand dunes at 100 m under sea level as proof of a post Younger-Dryas Black Sea lowstand *in* Yanko-Hombach, V., Buynevich, I., Chivas, A., Gilbert, A.S., Martin, R.E., and Mudie, P., eds., Extended Abstracts of the Second Plenary Meeting and Field Trip of IGCP 521 Project "Black Sea–Mediterranean corridor during the last 30 k.y.: Sea-level change and human adaptation," (20–28 August 2006, I.I. Mechnikov Odessa National University, Odessa, Ukraine): Odessa, Astroprint, p. 108–110.

Li, M.Z., and Amos, C.L., 1999, Field observations of bedforms and sediment transport thresholds of fine sand under combined waves and currents: Marine Geology, v. 158, p. 147–160, doi:10.1016/S0025-3227(98)00166-2.

Li, M.Z., Wright, L.D., and Amos, C.L., 1996, Predicting ripple roughness and sand resuspension under combined flows in a Shoreface environment: Marine Geology, v. 130, p. 139–161, doi:10.1016/0025-3227(95)00132-8.

McNinch, J.E., Trembanis, A.C., and Wells, J., 2006, A scour model for shipwrecks and marine artifacts—Developing and testing a predictive tool for nautical archaeologists: International Journal of Nautical Archaeology, v. 35, no. 2, p. 290–309, doi:10.1111/j.1095-9270.2006.00105.x.

McPhee-Shaw, E., 2006, Boundary-interior exchange: Reviewing the idea that internal-wave mixing enhances lateral dispersal near continental margins: Deep-sea Research. Part II, Topical Studies in Oceanography, v. 53, p. 42–59, doi:10.1016/j.dsr2.2005.10.018.

Miller, M.C., and Komar, P.D., 1980, Laboratory investigation of oscillation sand ripples: Journal of Sedimentary Petrology, v. 50, no. 1, p. 173–182.

Murray, A.B., and Thieler, E.R., 2004, A new hypothesis and exploratory model for the formation of large-scale inner-shelf sediment sorting and "rippled scour depressions": Continental Shelf Research, v. 24, no. 3, p. 295–315, doi:10.1016/j.csr.2003.11.001.

Neretin, L.N., Volkov, I.I., Böttcher, M.E., and Grinenko, V.A., 2001, A sulfur budget for the Black Sea anoxic zone: Deep-sea Research. Part I, Oceanographic Research Papers, v. 48, p. 2569–2593, doi:10.1016/S0967-0637(01)00030-9.

Nielsen, P., 1981, Dynamics and geometry of wave-generated ripples: Journal of Geophysical Research, v. 86, p. 6467–6472, doi:10.1029/JC086iC07p06467.

Oguz, T., and Besiktepe, S., 1999, Observations on the rim current structure, and CIW formation and transport in the western Black Sea: Deep-sea Research. Part I, Oceanographic Research Papers, v. 46, p. 1733–1753, doi:10.1016/S0967-0637(99)00028-X.

Oguz, T., Tugrul, S., Kideys, A.E., Ediger, V., and Kubilay, N., 2005, Physical and biogeochemical characteristics of the Black Sea *in* Robinson, A.R., and Brink, K.H., eds., The Sea: Cambridge, Harvard University Press, v. 14, Chapter 33, p. 1331–1369.

Osborne, P.D., and Vincent, C.E., 1993, Dynamics of large and small scale bedforms on a macrotidal shoreface under shoaling and breaking waves: Marine Geology, v. 115, p. 207–226, doi:10.1016/0025-3227(93)90051-V.

Özsoy, E., and Ünlüata, Ü., 1997, Oceanography of the Black Sea: a review of some recent results: Earth-Science Reviews, v. 42, p. 231–272, doi:10.1016/S0012-8252(97)81859-4.

Prothero, D., and Schwab, F., 2004, Sedimentary Geology, 2nd Ed.: New York, W.H. Freeman and Co., 557 p.

Richardson, M.D., and Traykovski, P., 2002, Real-time observations of mine burial at the Martha's Vineyard Coastal Observatory, *in* Scandrett, C., and Pearson, J., eds., Proceedings of the 5th International Symposium on Technology and the Mine Problem. Naval Postgraduate School, Monterey, California, 22–25 May 2002.

Riggs, S.R., Ambrose, W.G., Cook, J.W., Snyder, S.W., and Snyder, S.W., 1998, Sediment production on sediment-starved continental margins: the interrelationship between hardbottoms, sedimentological and benthic community processes, and storm dynamics: Journal of Sedimentary Research, v. 68, no. 1, p. 155–168.

Ryan, W.B.F., Pitman, W.C., III, Major, C.O., Shimkus, K., Moskalenko, V., Jones, G.A., Dimitrov, P., Görür, N., Sakınç, M., and Yüce, H., 1997, An abrupt drowning of the Black Sea shelf: Marine Geology, v. 138, p. 119–126, doi:10.1016/S0025-3227(97)00007-8.

Ryzhov, S.G., and Sedikova, L.V., 1999, "Komplexy X veka iz raskopok kvartala X (B) Severnogo raiona Khersonesa," in Khersonesskii Sbornik, vypusk X, p. 312–329. ("Tenth- century complexes based on the excavations of X (B) quarter of the northern area of Chersonesos," in Chersonesos Collection 10, p. 312–329.)

Schwab, W.C., and Molnia, B.F., 1987, Unusual bed forms on the north Aleutian shelf. Bristol Bay, Alaska: Geo-Marine Letters, v. 7, p. 207–215, doi:10.1007/BF02242773.

Schwab, W.C., Thieler, E.R., Allen, J.R., Foster, D.S., Swift, B.A., and Denny, J.F., 2000, Influence of inner-continental shelf geologic framework on the evolution and behavior of the barrier-island system between Fire Island Inlet and Shinnecock Inlet, Long Island, New York: Journal of Coastal Research, v. 16, no. 2, p. 408–422.

Soulsby, R., 1998, Dynamics of Marine Sands: A Manual for Practical Applications: London: Thomas Telford, 249 p.

Thieler, E.R., Brill, A.L., Cleary, W.J., Hobbs, C.H., and Gammisch, R.A., 1995, Geology of the Wrightsville Beach, North Carolina shoreface: Implications for the concept of shoreface profile of equilibrium: Marine Geology, v. 126, p. 271–287, doi:10.1016/0025-3227(95)00082-A.

Traykovski, P., Hay, A.E., Irish, J.D., and Lynch, J.F., 1999, Geometry, migration, and evolution of wave orbital ripples at LEO-15: Journal of Geophysical Research, v. 104, C1, p. 1505–1524, doi:10.1029/1998JC900026.

Traykovski, P., and Goff, J.A., 2003, Observations and modeling of large and small scale bedforms at the Martha's Vineyard Coastal Observatory, *in* Davis, R.A., Sallenger, A., and Howd P., eds., Coastal Sediments '03, Crossing Disciplinary Boundaries: Proceedings of the 5th International Symposium on Coastal Engineering and Science of Coastal Sediment Processes, World Scientific Publishing, Hackensack, New Jersey, 6000 p.

Trembanis, A.C., and P.A. Traykovski, 2005, Ripple and Morphologic Behavior of Sorted Bedforms: Eos (Transactions, American Geophysical Union) v. 86, no. 18, Joint Assembly Supplement, Abstract OS23B-01.

Trembanis, A.C., Wright, L.D., Friedrichs, C.T., Green, M.O., and Hume, T.M., 2004, The Effects of Spatially Complex Inner Shelf Roughness on Boundary Layer Turbulence and Current and Wave Friction: Tairua Embayment, New Zealand: Continental Shelf Research, v. 24, p. 1549–1571, doi:10.1016/j.csr.2004.04.006.

Trembanis, A.C., Friedrichs, C.T., Richardson, M., Traykovski, P.A., and Howd, P., 2007, Predicting Seabed Burial of Cylinders by Wave-Induced Scour: Application to the Sandy Inner Shelf off Florida and Massachusetts: IEEE Journal of Oceanic Engineering, v. 32, no. 1, p. 167–183, doi:10.1109/JOE.2007.890958.

Whitehouse, R., 1998, Scour at Marine Structures, A Manual for Practical Applications: London, Thomas Telford, 198 p.

Wiberg, P.L., and Harris, C.K., 1994, Ripple geometry in wave-dominated environments: Journal of Geophysical Research, v. 99, p. 775, doi:10.1029/93JC02726.

Wikramanayake, P.N., 1993, Velocity profiles and suspended sediment transport in wave-current flows [Ph.D. dissertation]: Massachusetts Institute of Technology, 285 p.

Wright, L.D., 1995, Morphodynamics of Inner Continental Shelves: Boca Raton, CRC Press, Inc., 256 p.

Wright, L.D., Kim, S.-C., and Friedrichs, C.T., 1999, Across-shelf Variations in Bed Roughness, Bed Stress and Sediment Transport on the Northern California Shelf: Marine Geology, v. 154, p. 99–115, doi:10.1016/S0025 3227(98)00106-6.

Yankovsky, A.E., and Chapman, D.C., 1995, Generation of mesoscale flows over the shelf and slope by shelf wave scattering in the presence of a stable, sheared mean current: Journal of Geophysical Research, v. 100, p. 6725–6742, doi:10.1029/94JC03339.

Yankovsky, A.E., and Chapman, D.C., 1996, Scattering of shelf waves by a spatially varying mean current: Journal of Geophysical Research, v. 101, p. 3479–3487, doi:10.1029/95JC02991.

Yankovsky, A.E., and Chapman, D.C., 1997, Anticyclonic eddies trapped on the continental shelf by topographic irregularities: Journal of Geophysical Research, v. 102, p. 5625–5639, doi:10.1029/96JC03452.

Manuscript Accepted by the Society 22 June 2010

Printed in the USA